J|A|C|S
ARTICLES
Published on Web 04/17/2002

In Situ EXAFS Analysis of the Temperature-Programmed Reduction of Cu-ZSM-5

Michael K. Neylon, Christopher L. Marshall,* and A. Jeremy Kropf

Contribution from the Argonne National Laboratory, Argonne, Illinois 60439

Received December 3, 2001

Abstract: High resolution in situ EXAFS during temperature-programmed reduction was performed on Cu-ZSM-5 to elucidate the state of copper under reaction conditions. Improvements in hardware and software allowed rapid acquisition of both XANES and EXAFS data during reduction, in particular, allowing observation of characteristic preedge features from various Cu oxidation states. EXAFS fitting and factor analysis of the normalized XANES edge were performed in an attempt to determine the number and type of Cu species present. The data suggests that initially only Cu^{2+} is present in two different locations on the zeolite; both states reduce to Cu^{1+} in both H_2 and CO, but under different conditions. Under H_2 conditions, migration of Cu^{1+} to Cu^0 clusters is observed at 450 °C, while no metallic state is observed during CO reduction.

Background

In recent years, a large number of catalytic systems have been investigated to address the problem of nitrogen oxide reduction from combustion sources to meet with increasing governmental regulations. Of interest is the copper-exchanged ZSM-5 system, which has been found to be active for both NO decomposition and the selective catalytic reduction of NO_x using light hydrocarbons.[1] The latter system has a high potential, although currently the performance of Cu-ZSM-5 under typical conditions for NO_x removal (particularly with high moisture content) is inadequate to meet expected requirements.

To better understand the nature of the Cu-ZSM-5 system, numerous attempts have been made to characterize the state of Cu in the ZSM-5 framework, particularly using methods such as X-ray photoelectron spectroscopy (XPS), Fourier transform infrared spectroscopy (FTIR), and electron paramagnetic resonance (EPR).[2−7] However, more promising results have been found using X-ray absorption fine structure spectroscopy (XAFS), since this method captures the local environment of the Cu species in addition to the oxidation state of Cu. Typically, most studies of Cu-ZSM-5 by XAFS[5−7] have occurred under ex situ conditions, in which the catalyst sample is treated in a reactive gas outside of the X-ray beamline and then moved into the beamline for analysis once the sample is cool. While this method can give satisfactory results, it requires time for sample transfer and conditioning, which can be a sparse commodity on many beamlines. Ideally, XAFS data can be collected in situ to acquire data rapidly and under changing conditions as specified by the experimenter.[8] This has been demonstrated, for example, in the temperature-programmed reduction of CuO on Al_2O_3.[9]

While others have also used in situ XAFS analysis of Cu-ZSM-5,[10−12] these studies appear to use longer data acquisition methods, thus limiting the number of temperature points examined. Recently, Iwasawa and co-workers have looked at the reduction of Cu-ZSM-5 in H_2 using in situ XAFS analysis with high-temperature resolution using an energy-dispersive monochromator.[13−15] While their results demonstrated the expected change of Cu from Cu^{2+} to Cu^{1+} to Cu^0, the intermediate Cu^{1+} state is not clearly observed. In particular, Cu^{1+} has a well-defined preedge feature around 8983 eV due to a 1s → 4p transition; this peak is very sharp.[6,11,16,17] In addition, Cu^{2+} may have a small preedge shoulder at 8987 eV due to a 1s → 3d transition. In Iwasawa's work, they collected XAFS data at 3-eV resolution, which can quite easily mask both of these features. Because their near-edge data did not resolve

* To whom correspondence should be addressed. E-mail: clmarshall@anl.gov.

(1) Shelef, M. *Chem. Rev.* **1995**, *95*, 209−225.
(2) Beutel, T.; Sárkány, J.; Lei, G. D.; Yan, J. Y.; Sachtler, W. M. H. *J. Phys. Chem.* **1996**, *100*, 845−851.
(3) Lamberti, C.; Bordiga, S.; Salvalaggio, M.; Spoto, G.; Zecchina, A.; Geobaldo, F.; Vliac, G.; Bellatreccia, M. *J. Phys. Chem. B* **1997**, *101*, 344−360.
(4) Kuroda, Y.; Kumashiro, R.; Yoshimoto, T.; Nagao, M. *Phys. Chem. Chem. Phys.* **1999**, *1*, 649−656.
(5) Kumashiro, R.; Kuroda, Y.; Nagao, M. *J. Phys. Chem. B* **1999**, *103*, 89−96.
(6) Bolis, V.; Maggiorini, S.; Meda, L.; D'Acapito, F.; Turnes Palomino, G.; Bordiga, S.; Lamberti, C. *J. Chem. Phys.* **2000**, *113*, 9248−9261.
(7) Turnes Palomino, G.; Fisicaro; P.; Bordiga, S.; Zecchina, A.; Giamello, E.; Lamberti, C. *J. Phys. Chem. B* **2000**, *104*, 4064−4073.
(8) Jacoby, M. *Chem. Eng. News* **2001**, *79*, 33−38.
(9) Fernández-García, M.; Rodríguez-Ramos, I.; Ferreira-Aparicio, P.; Guerrero-Ruiz, A. *J. Catal.* **1998**, *178*, 253−263.
(10) Márquez-Alvarez, C.; Rodríguez-Ramos, I.; Guerrero-Ruiz, A.; Haller, G. L.; Fernández-García, M. *J. Am. Chem. Soc.* **1997**, *119*, 2905−2914.
(11) Liu, D. J.; Robota, H. J. *J. Phys. Chem. B* **1999**, *103*, 2755−2765.
(12) Revel, R.; Bazin, D.; Seigneurin, A.; Barthe, P.; Dubuisson, J. M.; Decamps, T.; Sonneville, H.; Poher, J. J.; Maire, F.; Lefrancois, P. *Nucl. Instrum. Methods Phys. Res. B* **1999**, *155*, 183−188.
(13) Yamaguchi, A.; Shido, T.; Inada, Y.; Kogure, T.; Asakura, K.; Nomura, M.; Iwasawa, Y. *Catal. Lett.* **2000**, *68*, 139−145.
(14) Yamaguchi, A.; Inada, Y.; Shido, T.; Asakura, K.; Nomura, M.; Iwasawa, Y. *J. Synchrotron Rad.* **2001** *8*, 654−656.
(15) Yamaguchi, A.; Shido, T.; Inada, Y.; Kogure, T.; Asakura, K.; Nomura, M.; Iwasawa, Y. *Bull. Chem. Soc. Jpn.* **2001**, *74*, 801−808.
(16) Kau, L. S.; Spira-Solomon, D. J.; Penner-Hahn, J. E.; Hodgson, K. O.; Solomon, E. I. *J. Am. Chem. Soc.* **1987**, *109*, 6433−6442.
(17) Fulton, J. L.; Hoffmann, M. M.; Darab, J. G.; Palmer, B. J.; Stern, E. A. *J. Phys. Chem. A* **2000**, *104*, 11651−11663.

these peaks, they instead relied on changes in the coordination number of the first Cu−O shell to explain the presence of Cu^{1+}.

In this report, we discuss the use of in situ XAFS studies with rapid data acquisition and high-energy resolution to study the reduction of Cu-ZSM-5 in both H_2 and CO. Because of our ability to achieve a higher-energy resolution of at least 1.3 eV and high data-point density of at least 0.25 eV, the preedge features of Cu ions were very well defined. Because of this high definition, we were also able to use factor analysis to break down the XANES spectra into several components and analyze the state of Cu during the reductions. This report will provide insight into the reduction process of Cu-ZSM-5 and possible implications on the use of Cu-ZSM-5 for NO_x reduction.

Experimental Section

Copper-exchanged ZSM-5 was prepared by the typical ion-exchange method. Approximately 5 g of NH_4-ZSM-5 (Zeolyst, SiO_2/Al_2O_3 = 50) was exchanged multiple times with a 0.01 M $Cu(NO_3)_2$ solution (Aldrich). Each exchange was done by adding 10 mL of solution per gram of support, adjusting the pH of the solution to 8.0 using a dilute NH_4OH solution (Fisher), then stirring overnight. The slurry was then filtered, washed, and dried at 110 °C before being transferred to a calcination oven. The sample was heated in flowing air (AGA Gas, chromographic, ca. 300 cm^3/min) to 500 °C for 3 h. The Cu exchange level, based on a Cu^{2+}/Al^{+} ratio of 0.5, was estimated to be near 100%.

Temperature-programmed reduction (TPR) was done in a conventional setting using an Altamira AMI-1 flow system. Approximately 150 mg of sample was loaded into a 1/8-in. quartz U-tube and installed on the unit. A thermocouple was inserted into the middle of the sample bed. Flows and temperature were controlled by associated computer hardware, which also recorded all data from the system. Prior to the TPR run, the sample was dried at 500 °C in 30 cm^3/min Ar or He (depending on the makeup of the treatment gas) and then cooled back to room temperature. Either H_2/Ar (5.04%, AGA Gas) or CO/He (5.0%, AGA Gas) were passed over the sample at 30 cm^3/min, and the effluent was measured using a thermal conductivity detector. The temperature was held at room temperature for at least an hour before ramping to 800 °C at 3 °C/min.

In situ XAFS studies on the Cu K edge were done at the Materials Research Collaborative Access Team (MR-CAT) beamline at the Advanced Photon Source (APS), Argonne National Laboratory. The physical setup is similar to that which is outlined by Jacoby,[8] without post-analysis of the gas effluent, although future experiments can easily include gas chromatography or mass spectroscopy for effluent analysis. Approximately 40 mg of sample was loaded as a self-supporting wafer into a 1/2 in. metal holder (5/16 in. i.d.), which was then loaded into the center of a quartz sample tube (3/4 in. o.d.). The amount of sample used was calculated to optimize the signal across the Cu K edge compared with the absorption by Al and Si in the zeolite support. Both ends of the tube were sealed with stainless steel flanges that included globe valves for controlling flow and leak-tested Kapton windows. In addition, one flange cap was fitted with a thermocouple port; the end of a thermocouple was placed near the center of the sample holder. The sample was treated off-line in He (AGA Gas) at 500 °C for at least an hour before moving the sample cell onto the beamline. Prior to removing the sample from He, a slight positive pressure in the tube was induced to prevent air from entering the tube. The sample was placed in a table-mounted oven with supports at the ends and fixed into place.

A cryogenic double-crystal Si (111) monochromator was used along with a Rh-coated mirror to reduce harmonics. The experiment was run in transmission mode, with the X-ray beam passing through ionization chambers filled with N_2 before and after passing through the sample cell. In addition, a Cu foil reference spectrum for energy calibration was collected simultaneously with each scan using an additional ionization chamber.

Once the X-ray beam and sample were properly aligned, the gas lines to the sample tube were connected. Either H_2/He (4%, AGA) or CO/N_2 (1000 ppm, AGA) were used as reductants. The lines were sufficiently purged to prevent air from entering the gas lines before flow was initiated. The effluent gas was passed through a CO scrubber prior to venting into the hutch, and CO monitors were installed to verify that the CO levels in the hutch were within safe limits. The reductant gas flow at ca. 30 cm^3/min was allowed to stabilize for about 10 min before the temperature program was initiated. The temperature of the oven was ramped from room temperature to 600 °C at 3 °C/min.

For the CO TPR run, a full extended X-ray absorption fine-structure spectroscopy (EXAFS) scan from 8820 to 9700 eV at a step size of ca. 0.6 eV was collected approximately every 8 min. For the H_2 TPR run, installation of new hardware and software allowed the collection of both a XANES (X-ray absorption near edge structure) spectrum from 8890 to 9225 eV at a step size of ca. 0.25 eV and an EXAFS spectrum from 8820 to 9700 eV at ca. 1 eV every 5 min. The internal thermocouple temperature was monitored to verify the linearity of the heating ramp, which typically stabilized to the desired rate in less than 10 min upon the start of the ramp.

Data Analysis

Data analysis was performed by two methods. The first used standard methods to fit the extracted EXAFS function to obtain details on the local Cu environment. The energies were first adjusted using the reference copper foil. Background removal and edge-step normalization were performed using the AUTOBK program.[18] FEFFIT[19] was then used to fit the EXAFS function using paths for copper species (Cu, Cu_2O, and CuO) as generated by the FEFF (version 8.0) program.[20] The fitting was limited to a k range of 2.2−12.0 $Å^{-1}$, k^3 weighted, with modified Hanning windows, dk = 1.0 $Å^{-1}$, and an R range from 1.2 to 2.7 Å. Similar analysis was performed on reference samples of CuO and Cu metal to obtain S_0^2, the amplitude reduction factor, and subsequently, the coordination numbers of the fitted shells.

Three scattering paths were used to fit the data: a short Cu−O path consistent with the shortest Cu−O path in CuO (1.95 Å),[21] a long Cu−O path with length similar to that of the second neighbor Cu−O path in CuO (2.78 Å), and the first Cu−Cu path from metallic Cu at higher temperatures. For analysis, a Debye temperature model was used to simulate the Debye−Waller factor,[22] using a Debye temperature of 760 K for the two Cu−O shells and 310 K for the Cu−Cu shell. The energy shifts for each shell were found to remain unchanged over the temperature range and were subsequently set to constant values (−3.5 eV for Cu−O shells, −10.0 eV for Cu−Cu). Thus, fitting was only performed on the coordination number and the radial distance of each shell, for a maximum of six variables. However, not every shell was used for every fit, and thus the total number of variables was typically less than six. The number of independent measurements N for a single spectrum analyzed by Fourier transform can be calculated from

(18) Ravel, B. *J. Synchrotron Rad.* **2001**, *8*, 314−316.
(19) Stern, E. A.; Newville, M.; Ravel, B.; Yacoby, Y.; Haskel, D. *Physica B* **1995**, *208*−*209*, 117−120.
(20) Ankudinov, A. L.; Ravel, B.; Rehr, J. J.; Conradson, S. D. *Phys. Rev. B* **1998**, *58*, 7565−7576.
(21) Åsbrink, S.; Norrby, L. J. *Acta Crystallogr. B* **1970**, *26*, 8−15.
(22) Lee, P. A.; Pendry, J. B. *Phys. Rev. B* **1975**, *11*, 2795−2811.

$$N = \frac{2 \cdot \Delta k \cdot \Delta R}{\pi} + 1$$

where Δk is the k range over which the Fourier Transform was performed and ΔR is the R range for the same.[23,24] For the ranges used, this expression gives a maximum of 12 variable parameters, which is higher than the actual number of variables we used. The amplitude factor for each shell was compared with the measured amplitudes from CuO powder and Cu foil reference materials and was used to generate the coordination number for each shell.

The second method used to analyze the data involved the use of factor analysis on the XANES data from the H_2 TPR run. The XANES region was selected for factor analysis since it is relatively insensitive to the temperature-induced changes in the EXAFS Debye−Waller factor. First, the energy of all of the XANES spectra were calibrated to the same energy grid using the reference Cu foil transmission spectrum channel to within 0.05 eV. Spectra were normalized using a two-step process. First, a first-order polynomial fit in the preedge region from 8890 to 8937 eV was performed to determine the baseline signal. The spectra were then normalized to an edge step of 1 by extracting a zero-order fit over the range 9087−9225 eV to the edge energy 8987 eV. Then, cubic splines were used to convert each spectrum to a constant energy grid from 8960 to 9030 eV at 0.125-eV increments. The factor analysis was performed using methods similar to those from Malinowski.[25] The normalized discrete data were collected in a matrix, and singular value decomposition was used to find the associated eigenvalues and eigenvectors. Using empirical selection rules as discussed below, either three or four eigenvalues and eigenvectors were selected to be the basis set for the system. While, ideally, for XANES analysis, pure phases of the species in question should be selected, the pure Cu states have significantly different XANES behavior than the zeolite counterparts, and would drastically affect the factor analysis results. Instead, iterative key set factor analysis (IKSFA)[25] was used to determine which of the initial XANES data sets were most fundamental, and the other data in the set were fitted using a least-squares analysis on a linear sum of these fundamental vectors.

Results

Temperature-Programmed Reduction. The TCD signal in terms of hydrogen consumption from H_2 TPR of Cu-ZSM-5 is shown in Figure 1a. This trace is similar to other TPR results in the literature;[2,26,27] a low-temperature peak between 170 and 210 °C in which both CuO may be reduced in one step to Cu metal, and where isolated Cu^{2+} ions may reduce to Cu^{1+}, and a high-temperature peak where Cu^{1+} is reduced to Cu metal. These assignments are tentative and will be clarified later. Further analysis with PEAKFIT[28] shows that the low-temperature peak is a summation of two peaks at 175 and 205 °C.

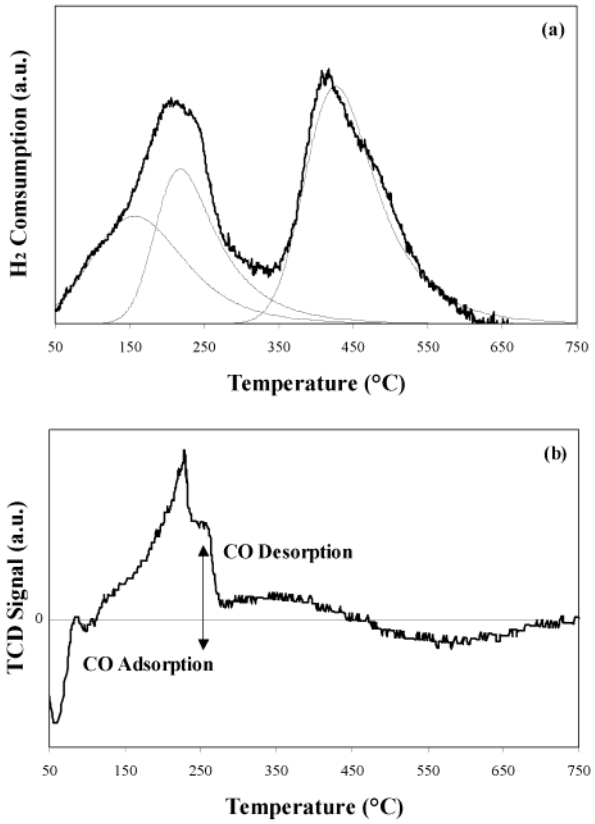

Figure 1. (a) Hydrogen generation trace during the temperature-programmed reduction of Cu-ZSM-5 in 5% H_2/Ar at 3 °C/min. (b) TCD signal trace during the temperature-programmed reduction of Cu-ZSM-5 in 5% CO/He at 3 °C/min.

While synthesis conditions were used to minimize the amount of CuO clusters, one of these low-temperature peaks may be a result of CuO in the sample.

The TCD trace from CO TPR is shown in Figure 1b. Initially, there is adsorption and successive desorption of the CO at temperatures below 150 °C. At around 500 °C, there is a very slow consumption of CO, attributed tentatively to the reduction of Cu ions. Carbon monoxide is a sufficiently weak reductant such that it cannot reduce CuO at temperatures used here but can easily reduce isolated Cu species.

XANES Spectra. The normalized in situ XANES data collected during the H_2 TPR of Cu-ZSM-5 are shown in Figure 2. Clearly, features associated with the various oxidation states of Cu can be observed during the entire TPR process; most importantly, a preedge feature near 8983 eV can be seen to develop and then disappear with increasing temperature. This preedge feature is a clear indication of the 1s-to-4p transition in Cu^{1+}. Because of the small step size used, this preedge feature is defined by at least 10 data points in all spectra when present; in the XANES TPR study of Isawama, this preedge feature was not seen due to the lower-energy resolution of the energy dispersive XAFS beamline.[14,15] In addition to this preedge feature, the presence of Cu^{2+} can be observed at lower temperatures, as indicated by the shoulder at ca. 8987 eV, and Cu^0 at the higher temperature due to the splitting of the postedge peak. The transformation of Cu^{2+} to Cu^{1+} appears to initiate as low as 100 °C, with the maximum Cu^{1+} content at 380 °C, coinciding with the formation of Cu^0. The rate of growth of the Cu^{1+} preedge peak with respect to temperature would seem

(23) Brillouin, L. *Science and Information Theory*; Academic Press: New York, 1962.
(24) Stern, E. A. *Phys. Rev. B* **1993**, *48*, 9825−9827.
(25) Malinowski, E. R. *Factor Analysis in Chemistry*, 2nd ed.; John Wiley and Sons: New York, 1991.
(26) Yan, J. Y.; Lei, G. D.; Sachtler, W. M. H.; Kung, H. H. *J. Catal.* **1996**, *161*, 43−54.
(27) Bulánek, R.; Wichterlová, B.; Sobalík, Z.; Tichý, J. *Appl. Catal. B* **2001**, 31, 13−25.
(28) *PeakFit*, version 4; Jandel Scientific Software: San Rafael, CA, 1995.

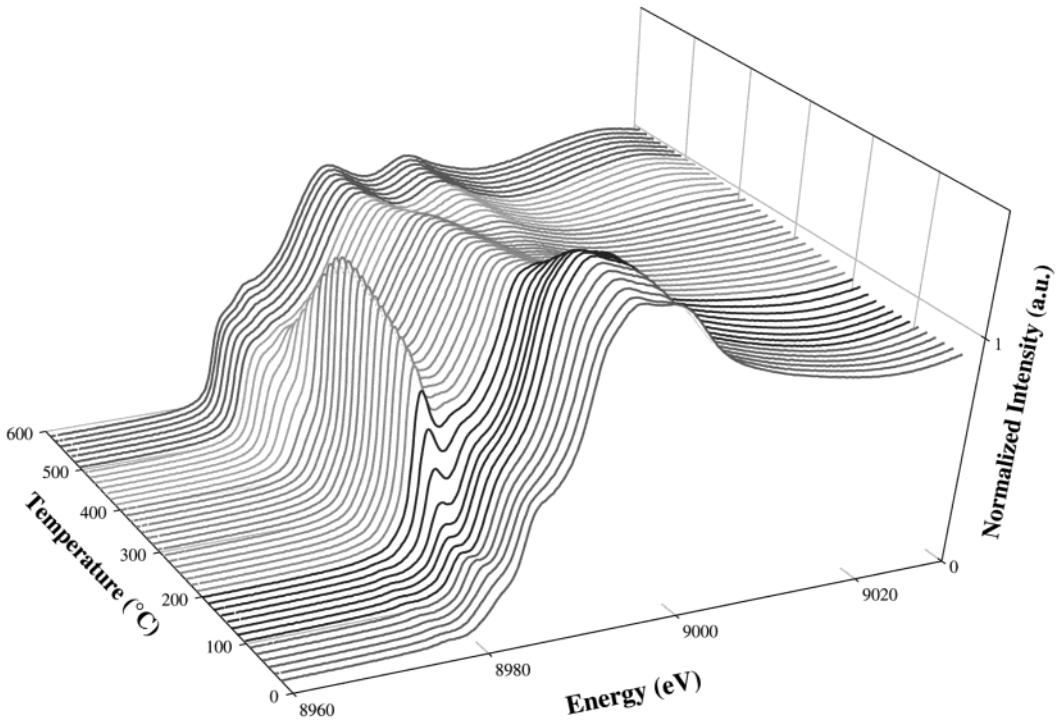

Figure 2. Normalized XANES spectra across the Cu K edge collected during the temperature-programmed reduction of Cu-ZSM-5 in 5% H_2/He at a rate of 3 °C/min.

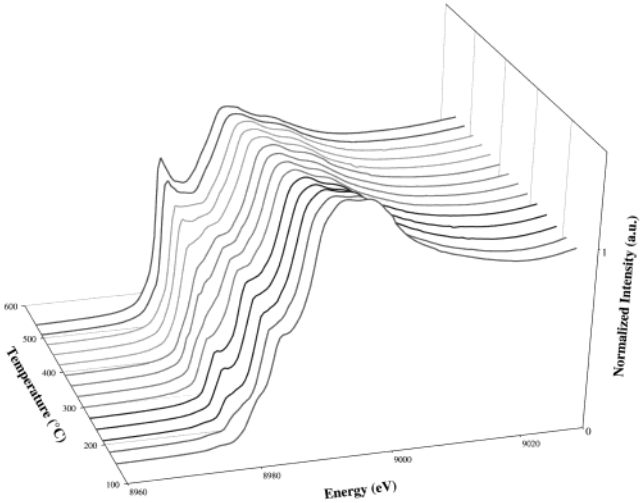

Figure 3. Normalized XANES spectra across the Cu K edge collected during the temperature-programmed reduction of Cu-ZSM-5 in 1000 ppm CO/N_2 at a rate of 3 °C/min.

to indicate that there are two rates of formation of Cu^{1+}: rapid formation from 120 to 200 °C and somewhat slower formation from 225 to 380 °C. At 600 °C, while the XANES spectrum is mostly Cu^0, there are indications from the preedge features that some Cu^{1+} still is present on the sample.

While the CO TPR data shown in Figure 3 lacks the resolution in both temperature and energy demonstrated by the H_2 TPR data (as explained earlier), it is nevertheless still useful. There appears to be a very slow introduction of Cu^{1+} as shown by a preedge feature near 8983 eV into the system above 200 °C, with a strong development of this peak at temperatures near 450 °C. Simultaneously, there is a slow drop in the magnitude of the first postedge peak at 8993 eV and the preedge feature at 8987 eV throughout this temperature range. At no time does Cu metal appear to be formed. These data agree with the weak reduction potential of CO on Cu-ZSM-5 catalysts.

EXAFS Analysis. The Fourier transform of the EXAFS data for the H_2 TPR of Cu-ZSM-5 is shown in Figure 4. The fitted parameters along with error estimates are presented in Table 1. The coordination numbers of each shell are presented in Figure 5a. The fits were able to account for all but 5% of the variance in the data, even in the worst cases. The goodness-of-fit parameter $\mathcal{R}$ calculated from the sum of the squares of the difference between the experimental data and the fit, and normalized to the amplitude of the data, is also given in Table 1. Initially, there is a large contribution from Cu−O bonds at 1.95 Å as well as from a longer Cu−O bond at 2.85 Å. There is also a set of shells in the 3.5−5.0 Å range; while additional paths from CuO and Cu_2O were used to try to fit these paths, no successful model could be discovered. Previous EXAFS studies in the literature suggest that the shells in this region are associated with scattering from Cu−O−Cu bridges that can easily exist in Cu-ZSM-5 and other exchanged zeolites.[7,29−32] Note that no Cu−Cu shell could be fitted in the 1.2−5.0 Å range at low temperatures, which suggests that the Cu exists mostly as isolated Cu species on the zeolite framework, as opposed to small CuO particles. For comparison, several Cu-ZSM-5 species that were drastically overexchanged were examined separately under EXAFS as shown in Figure 6; also shown is pure CuO. The strong presence of a Cu−Cu shell and additional shells at $R > 3$ Å in these materials indicate the presence of long-range order from CuO or Cu_2O cluster formation. In contrast, these cluster features are not present on

(29) Grünert, W.; Hayes, N. W.; Joyner, R. W.; Shpiro, E. S.; Rafiq, M.; Siddiqui, H.; Baeva, G. H. *J. Phys. Chem.* **1994**, *98*, 10832−10846.
(30) Kuroda, Y.; Yoshikawa, Y.; Konno, S. I.; Hamano, H.; Maeda, H.; Kumashiro, R.; Nagao, M. *J. Phys. Chem.* **1995**, *99*, 10621−10628.
(31) Kuroda, Y.; Maeda, H.; Yoshikawa, Y.; Kumashiro, R.; Nagao, M. *J. Phys. Chem. B* **1997**, *101*, 1312−1316.
(32) Huang, Y. J.; Wang, H. P. *J. Phys. Chem. A* **1999** *103*, 6514−6516.

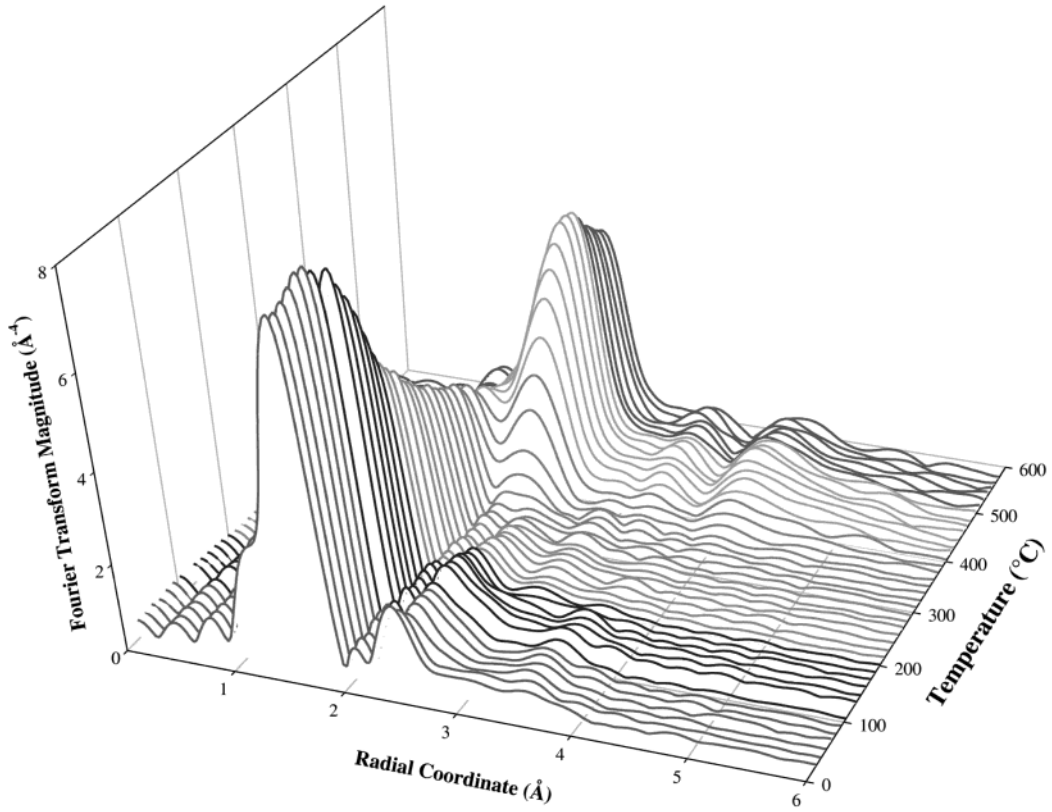

Figure 4. Radial distribution plot collected on the EXAFS spectra collected at the Cu K edge during the temperature-programmed reduction of Cu-ZSM-5 in 5% H_2/He at a rate of 3 °C/min. Radial positions have not been corrected for phase shift.

Table 1. EXAFS Fitting Parameters for Selected Temperatures during H_2 TPR Reduction of Cu-ZSM-5

	Cu–O first shell			Cu–O second shell			Cu–Cu			
temp °C	N[a]	R[b]	σ^2 [c]	N[a]	R[b]	σ^2 [c]	N[a]	R[b]	σ^2 [c]	$\mathcal{R}$ [d]
25	4.8 ± 0.5	1.95 ± 0.01	0.51	3.0 ± 0.5	2.85 ± 0.01	0.75	n.f.[e]	n.f.	n.f.	0.8
100	5.4 ± 0.6	1.96 ± 0.01	0.60	2.7 ± 0.5	2.91 ± 0.02	0.89	n.f.	n.f.	n.f.	0.6
200	3.9 ± 0.4	1.94 ± 0.01	0.72	1.9 ± 0.7	2.85 ± 0.04	1.07	n.f.	n.f.	n.f.	1.9
300	2.8 ± 0.3	1.96 ± 0.01	0.84	0.3 ± 0.5	2.85 ± 0.08	1.27	n.f.	n.f.	n.f.	3.9
400	1.6 ± 0.2	1.97 ± 0.01	0.98	n.f.	n.f.	n.f.	4.0 ± 0.3	2.51 ± 0.01	1.67	4.1
500	0.3 ± 0.2	1.97 ± 0.02	1.12	n.f.	n.f.	n.f.	8.2 ± 0.3	2.51 ± 0.01	1.94	0.9
600	0.3 ± 0.2	1.97 ± 0.02	1.23	n.f.	n.f.	n.f.	8.3 ± 0.4	2.50 ± 0.01	2.22	1.4

[a] Coordination number. [b] Bond length (Å). [c] Debye−Waller factor ($\times 10^{-2}$ Å^2) calculated from the Debye temperature model as described in the text. [d] Goodness-of-fit parameter ($\times 10^{-2}$). [e] n.f. = not fitted at these conditions.

the ca. 100% exchanged Cu-ZSM-5 sample used in this study, demonstrating the isolation of the Cu species. The initial coordination number of 4.8 for the first Cu−O shell is larger than the expected value of 4 for CuO, but previous researchers have found coordination numbers up to 6 for Cu−O in ZSM-5 when charge-balanced by hydroxyl groups.[7,29,33]

As the temperature was increased, the amplitude of the Cu−O shells declined at about the same rate. As with the XANES data, there appears to be two different rates—a fast change from 150 to 200 °C, followed by a slower rate up to 325 °C. At this temperature, the second Cu−O disappeared, with the formation of Cu−Cu at ca. 2.50 Å. The first Cu−O shell continued to diminish as the Cu−Cu shells appeared between 300 and 500 °C, with only small changes above 500 °C. Note that there is still a small contribution from the first Cu−O shell even at 600 °C, suggesting that there may still be isolated Cu species on the sample, also in agreement with the small Cu^{1+} preedge feature observed in the XANES spectra. In addition, there is a formation of additional Cu−Cu shells typically associated with multiple scattering effects in the range from 3.5 to 5 Å at increasing temperatures. Using an estimation technique from Greegor and Lytle[34] and a more detailed fit of the higher-order Cu−Cu shells with the high-temperature spectra, the average size of these copper clusters appears to be near 6 Å, assuming spherical particles. Because Cu appears to only be present as isolated species at the start of the run, this suggests that Cu can migrate on the surface to form Cu clusters at temperatures above 400 °C. The estimated particle size agrees well with the typical channel size in ZSM-5 (ca. 5.5 Å), suggesting that Cu migrates only inside the channels of ZSM-5. Previous researchers have observed by transmission electron microscopy the formation of Cu on the outside of the porous support.[9,13]

For the CO TPR, the only observed shells between 1.2 and 2.7 Å are the two Cu−O shells from above, as shown in Figure 5b. Path parameters at selected temperatures from fitting are tabulated in Table 2. No Cu−Cu shell was observed at any

(33) Yamashita, H.; Matsuoka, M.; Tsuji, K.; Shioya, Y.; Anpo, M.; Che, M. *J. Phys. Chem.* **1996**, *100*, 397−402.

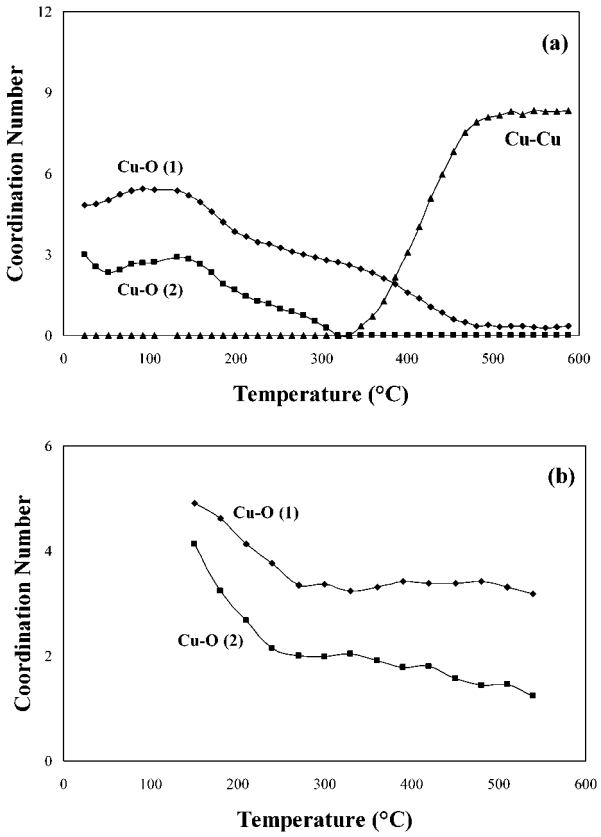

Figure 5. (a) Coordination numbers of the first and second Cu−O shells and the first Cu−Cu shell as a function of temperature, as fitted from the EXAFS spectra during H_2-TPR. (b) Coordination numbers of the first and second Cu−O shells as a function of temperature, as fitted from the EXAFS spectra collected during CO-TPR.

temperature in this study. The coordination of the first shell is comparable with the coordination of the first shell from H_2 TPR, albeit at a higher temperature, while the second shell coordination is significantly higher. However, with moderate temperatures, the coordination numbers drop significantly to levels similar to that found during H_2 TPR. Given that desorption of CO was observed during TPR in this temperature range, the higher coordination numbers here may be due to the presence of CO on the sample, which agrees with previous results on the ease of CO adsorption on Cu-ZSM-5.[35−38] Since C and O are only two elements apart on the periodic table, they have similar EXAFS phase shifts and backscattering amplitude functions. Therefore, it is very difficult to distinguish between the two, especially if the bond length is similar. While, in some cases, it may be possible to model Cu−C bond contributions that arise from CO adsorption, the EXAFS data collected for this run do not extend to high enough k values to distinguish Cu−O and Cu−C contributions. At high temperatures, the first Cu−O shell remains unchanged while there is a continued decrease in the second shell, suggesting that some reduction of Cu^{2+} to Cu^{1+} is taking place.

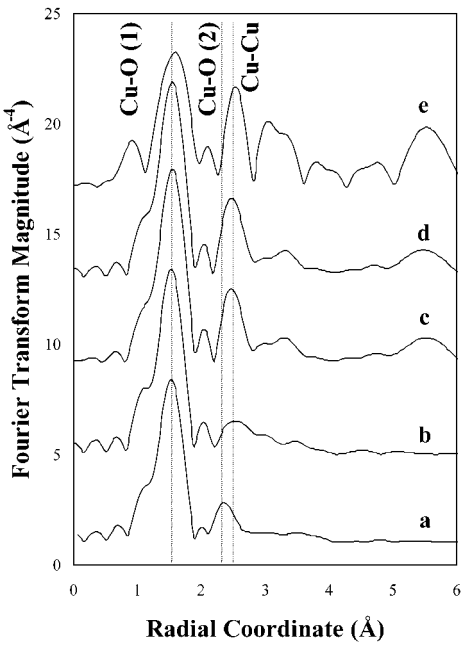

Figure 6. Fourier transform magnitude for several Cu species ($\Delta k = 2.2-12.0$ Å^{-1}, dk = 1.0 Å^{-1}, k^3 weight). (a) Cu-ZSM-5 used throughout this study. (b) Cu-ZSM-5 at ca. 125% exchange. (c) Cu-ZSM-5 at ca. 200% exchange. (d) Cu-ZSM-5 at ca. 300% exchange. (e) pure CuO. Lines indicate the positions of the two Cu−O shells and the first Cu−Cu shell in CuO. All data were collected at room temperature.

Table 2. EXAFS Fitting Parameters for Selected Temperatures during CO TPR Reduction of Cu-ZSM-5

temp	Cu–O first shell			Cu–O second shell			
°C	N[a]	R[b]	σ^2[c]	N[a]	R[b]	$\Delta\sigma^2$[c]	$\mathscr{R}$[2 d]
150	4.9 ± 0.6	1.94 ± 0.01	0.69	4.1 ± 0.8	2.84 ± 0.02	1.03	1.9
300	3.3 ± 0.4	1.95 ± 0.01	0.84	2.0 ± 0.5	2.82 ± 0.03	1.26	1.7
450	3.4 ± 0.4	1.95 ± 0.01	1.00	1.8 ± 0.9	2.84 ± 0.05	1.56	4.1
570	3.2 ± 0.4	1.96 ± 0.01	1.21	1.2 ± 1.1	2.85 ± 0.09	1.80	7.2

[a] Coordination number. [b] Bond length (Å). [c] Debye−Waller factor ($\times 10^{-2}$ Å^2) calculated from the Debye temperature model as describe in the text. [d] Goodness-of-fit parameter ($\times 10^{-2}$).

The values obtained for bond lengths for the first Cu−O shell and Cu−Cu from EXAFS fitting in this study agree well with previous results in the literature, both other EXAFS studies on Cu-ZSM-5[7,14,15,31] as well as results from computational chemistry for Cu-ZSM-5 or related clusters.[39−43] Of note is the second Cu−O shell at 2.85 Å, consistent with the second Cu−O path in CuO, which is typically not observed in previous literature on Cu-ZSM-5. As shown in Figure 6, this feature can be easily obscured by the presence of Cu−Cu bonds from small Cu−O clusters and, thus, may be undetectable by previous work. In addition, most previous papers focus strictly on the first Cu−O and Cu−Cu shells, as well as a Cu−O−Cu contribution at ca. 3.5 Å, and attempts at fitting the Cu−O shell at 2.85 Å have not been mentioned. Grünert et al.,[29] in studying various Cu-ZSM-5 samples that have been mildly reduced as to retain some isolated Cu character but removing much of a CuO-like species,

(34) Greegor, R. B.; Lytle, F. W. *J. Catal.* **1980**, *63*, 476−486.
(35) Kuroda, Y.; Yoshikawa, Y.; Emura, S.; Kumashiro, R.; Nagao, M. *J. Phys. Chem. B* **1999**, *103*, 2155−2164.
(36) Bordiga, S.; Turnes Palomino, G.; Arduino, D.; Lamberti, C.; Zecchina, A.; Otero Areán, C. *J. Mol. Catal. A* **1999**, *146*, 97−106.
(37) Zecchina, A.; Bordiga, S.; Turnes Palomino, G.; Scarano, D.; Lamberti, C.; Salvalaggio, M. *J. Phys. Chem. B* **1999**, *103*, 3833−3844.
(38) Lamberti, C.; Turnes Palomino, G.; Bordiga, S.; Berlier, G.; D'Acapito, F.; Zecchina, A. *Angew. Chem., Int. Ed.* **2000**, *39*, 2138−2141.
(39) Schneider, W. F.; Hass, K. C.; Ramprasad, R.; Adams, J. B. *J. Phys. Chem.* **1996**, *100*, 6032−6046.
(40) Hass, K. C.; Schneider, W. F. *J. Phys. Chem.* **1996**, *100*, 9292−9301.
(41) Trout, B. L.; Chakraborty, A. K.; Bell, A. T. *J. Phys. Chem.* **1996**, *100*, 4173−4179.
(42) Teraishi, K.; Ishida, M.; Irisawa, J.; Kume, M.; Takahashi, Y.; Nakano, T.; Nakamura, H.; Miyamoto, A. *J. Phys. Chem. B* **1997**, *101*, 8079−8085.
(43) Rice, M. J.; Chakraborty, A. K.; Bell, A. T. *J. Phys. Chem. B* **2000**, *104*, 9987−9992.

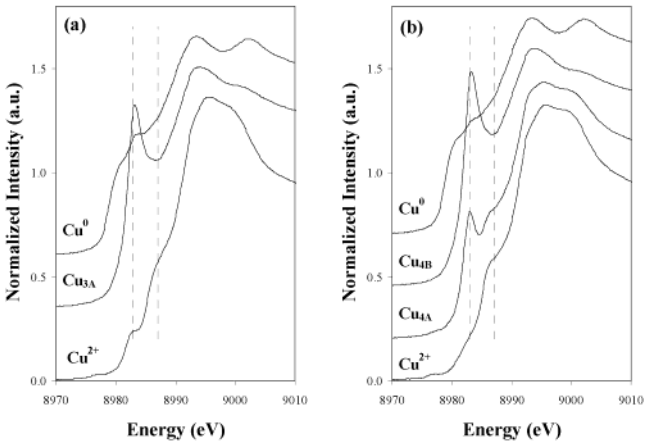

Figure 7. Key basis spectra as determined from factor analysis of the XANES data collected during H_2-TPR for Cu-ZSM-5. (a) Basis set for the three-component fit. (b) Basis set for the four-component fit.

observe a Cu−O shell near 2.95 Å which they attribute to Cu−O−Cu bridging species. On the basis of molecular simulations, this Cu−O bond length is on an order similar to that of the Cu−O length predicted for Cu−O−Cu bridging species between two adjacent rings in the zeolite structure.[42] Further analysis in conjunction with other shells in Cu-ZSM-5 may be necessary to fully describe this shell. Also, as seen in Tables 1 and 2, the length of these bonds do not vary much over the course of reduction; only the second Cu−O shell shows any appreciable change, but no more than 0.05 Å from the average value. While it would be expected that during reduction, the lengths of these bonds would change,[7] the coordination of the isolated Cu species to the zeolite may be sufficiently strong such that the Cu ions remain fixed in place on the surface of the zeolite until strong reduction conditions (such as in H_2 above 400°) are encountered, at which point the Cu ions become migratory and form Cu clusters.

Factor Analysis. Factor analysis of the H_2 TPR data showed that no less that three components were present in the various XANES spectra. However, three components only accounted for 99.9% of the variance in the data; using a fourth component resulted in a 99.99% accounting. Using empirical methods, it was determined that using five or more components was over-compensating for the experimental error. For comparison, both a three-component and four-component fit were investigated. For both cases, IKSFA resulted in a low-temperature (<100 °C) and a high-temperature (>500 °C) component. The remaining one or two components, respectively, were found in the moderate temperature range of 200−300 °C. We have assigned the lowest-temperature component as predominantly Cu^{2+}, and the highest-temperature component as predominantly Cu^0, given the similarity of these spectra to expected spectra for those oxidation states (Figure 7). The intermediate peaks we have assigned as either Cu_{3A} or Cu_{4A} and Cu_{4B} for the intermediate states for either three- or four-component fits, respectively; these states appear to be related to Cu^{1+}, as the Cu^{1+} preedge feature is predominate in each, but may have some Cu^{2+} nature as well.

Examining the spectra that were found to be the key basis vectors as shown in Figure 7 gives more insight to the compositions at these states. Unsurprisingly, the first spectrum in either fit yields only the expected features of Cu^{2+}, the small shoulder near 8987 eV with a very small contribution from the

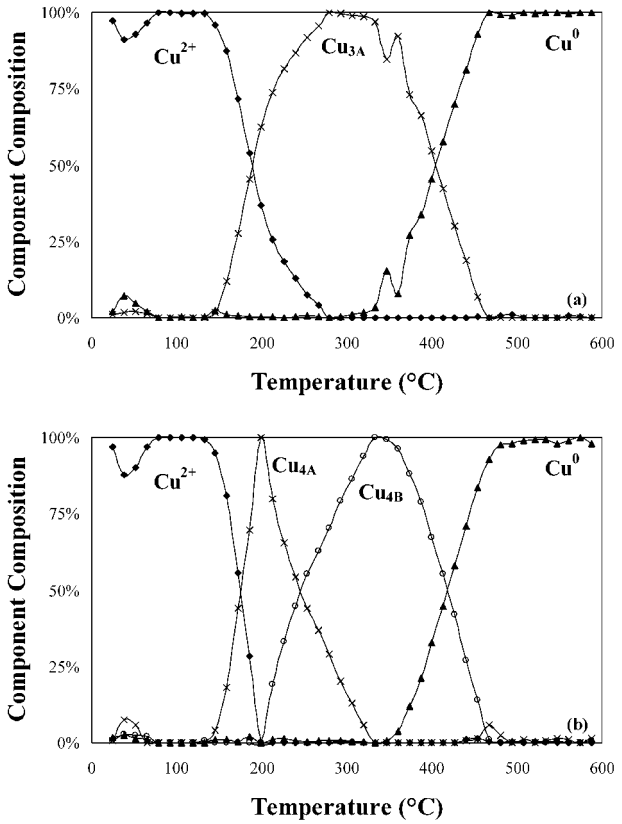

Figure 8. Phase composition of each XANES spectra during H_2-TPR of Cu-ZSM-5 as determined from factor analysis. (a) Compositions determined using a three-component fit. (b) Compositions determined using a four-component fit.

preedge feature of Cu^{1+}. The high-temperature spectrum is clearly Cu^0. In the case of the three-component fit, the intermediate phase appears to be mostly Cu^{1+}, based on the strong preedge features and the lack of Cu^{2+} features in both the pre- and postedges, though these may be obscured by the Cu^{1+} features. On the other hand, the intermediates in the four-component fit show distinct phases. In Cu_{4A}, there is evidence for both a small amount of Cu^{1+} as well as Cu^{2+} in the preedge feature range; the postedge spectra of these materials indicate that no metallic Cu−Cu bonds are present at this point. The component Cu_{4B}, alternatively, shows a very strong Cu^{1+} contribution in the preedge, which might be masking the preedge Cu^{2+} feature. However, the second postedge peak at 8999 eV, present in the first two components, is no longer present; instead, a peak at 9003 eV has formed that is similar to that of Cu^0. This would suggest that there is no Cu^{2+} left in the system by this point, and Cu_{4B} is mostly Cu^{1+} with some small amounts of Cu^0. Additionally, one can argue that Cu_{3A} and Cu_{4B} represent the same state on the basis of these data.

Using the selected component states, the remaining XANES spectra were fitted to a linear combination of these states to determine the composition of each state, as shown in Figure 8 for both the three- and four-component fits. Note that because no true reference materials were used, the composition of the basis components appear to be only composed of one phase, but may actually be a composition of true multiple phases, as indicated by the analysis of the XANES structure. However, these compositions can still be used to observe the stepwise transformation of the spectra between the three or four states.

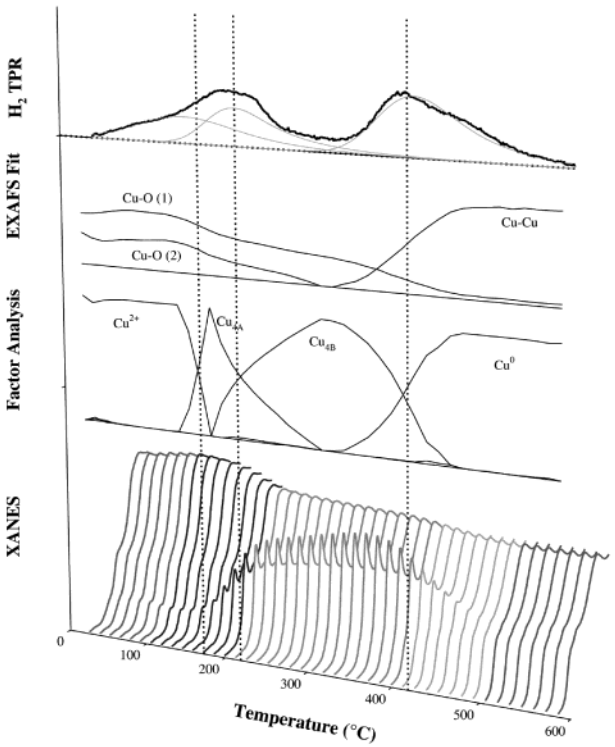

Figure 9. Combined data representation of the H_2-TPR trace, EXAFS data analysis, XANES factor analysis, and preedge features during the H_2-TPR of Cu-ZSM-5.

Discussion

The results from ex situ TPR (Figure 1a), EXAFS fitting (Figure 5a), the four-component factor analysis (Figure 8b), and a visual representation of the XANES edge region (Figure 2) are shown in Figure 9. From the TPR, three distinct transitions can be isolated at 175, 210, and 410 °C. The location of these points agree with changes in the preedge Cu^{1+} feature as seen from the XANES, in particular, in the range of fast Cu^{1+} formation, slow Cu^{1+} formation, and Cu^{1+} disappearance, respectively. These temperatures also agree with the changes in the coordination numbers from the EXAFS for the initial fast and slow reduction of the number of Cu−O bonds and the formation of Cu−Cu bonds, respectively. When compared to the four-component factor analysis data, these temperatures also occur near the transition between two of the components. There is strong agreement between all four analyses, suggesting that the results from ex situ studies can be improved with in situ EXAFS analysis, with good agreement between temperature-related events.

The formation of CuO is believed to be detrimental to the function of Cu-ZSM-5 for NO_x removal, given that the activity of Cu-ZSM-5 for SCR increases as the Cu exchange level approaches 100%, but then remains constant or drops with over-exchanged samples.[1,44,45] However, the exact mechanism and nature of the active sites is still in question, and results have been published that show the contrary, that CuO clusters may be necessary for the SCR reaction in conjunction with isolated Cu sites.[10] Typically, care is taken to try to prevent the formation of CuO, although it may still be formed with exchange levels as low as 40%.[2] On the basis of the analysis of our samples, we appear to have been able to synthesize Cu-ZSM-5 near 100% exchange with very low amounts of CuO clusters, relative to the amount of isolated Cu species. X-ray diffraction of the sample showed no change from the parent ZSM-5 structure, although it would be expected that CuO clusters in the ZSM-5 framework would be smaller than 20 Å and thus be virtually undetectable by diffraction. Because two low-temperature peaks are present from the H_2-TPR, these may be related to two different types of isolated Cu species. The analysis of the EXAFS spectra showed that fitting to the longer-range order, particularly the Cu−Cu paths, of either CuO or Cu_2O could not be performed; instead, only the nearest Cu−O bonds were necessary. Comparison of the Fourier transforms of this material with overexchanged materials showed that the expected first Cu−Cu bond was not present in a measurable amount. In addition, the reduction of CuO at low temperatures in hydrogen around 200 °C should result in Cu metal clusters, and again, these were not observed until 350 °C. Thus, while CuO may be present on this catalyst, it remained undetected by our results.

The data in Figure 9 clearly demonstrates the fate of Cu on ZSM-5 during the reduction of H_2 TPR. Initially, most of the Cu appears to be present as isolated Cu^{2+} species, with possible small amounts of Cu^{1+}. At temperatures around 175−205 °C, Cu^{2+} can be reduced by H_2 to isolated Cu^{1+} species. This reduction continues until near 375 °C, at which temperature Cu^{1+} reduction starts and continues until 500 °C. As Cu^{1+} is reduced to the metallic state, there appears to be associated migration of the metal species into small clusters inside the zeolite. There appear to be no further reduction or migration events after 500 °C. However, there appears to be a small fraction of ionic Cu species, even at temperatures above 500 °C, as the short Cu−O bond never fully disappears. This bond may be from Cu species isolated on the zeolite matrix (possibly inside the zeolite walls or the nonchannel openings) or from the anchoring of the Cu clusters to the zeolite.

Using IKSFA, we found that there may be three or four species present during the reduction of Cu-ZSM-5. Isolated Cu^{2+} and Cu metal cluster species are readily apparent from the data. However, deciphering what the remaining states are can be difficult, particularly without the help of zeolite-supported standards. Considering the case of only three components, we can easily claim that the third component, Cu_{3A}, is isolated Cu^{1+}, which is in agreement with the reduction of the coordination number from fitting the EXAFS function. However, H_2 TPR demonstrates that there were three reduction events; if exactly three Cu species were possible on Cu-ZSM-5, it would be expected to see only two reduction events. Thus, we are inclined to look at the four-component system in more detail.

Previous researchers have suggested that there are at least two possible positions for Cu ions to sit on ZSM-5, typically defined by differences in the local zeolite structure. For example, Wichterlová et al.[27,46] have shown, using UV−vis, TPR, and FT-IR, that two distinct sites appear to exist for Cu ions; the relative ratio of these sites is a strong function of the Si/Al ratio of the ZSM-5 framework. Yan et al.,[26] Carl and Larsen,[47] and Gómez et al.[48] have all used electron paramagnetic resonance

(44) Kharas, K. C. C. *Appl. Catal. B* **1993**, *2*, 207−224.
(45) Torre-Abreu, C.; Ribeiro, M. F.; Henriques, C.; Ribeiro, F. R. *Appl. Catal. B* **1997**, *11*, 383−401.
(46) Dèdeèek, J.; Wichterlová, B. *J. Phys. Chem.* **1994**, *98*, 5721−5727.
(47) Carl, P. J.; Larsen, S. C. *J. Phys. Chem. B* **2000**, *104*, 6568−6575.
(48) Gómez, S. A.; Campero, A.; Martínez-Hernández, A.; Fuentes, G. A. *Appl. Catal. A* **2000**, *197*, 157−164.

to observe Cu^{2+} on ZSM-5 in at least two states, as a square planar and a square pyramidal coordination; unfortunately, Cu^{1+} is EPR silent, and thus similar analysis cannot be performed on this species.

Additionally, the energetics of Cu ions on ZSM-5 zeolite have been investigated using computational chemistry, leading to results that generally agree with the concept of two sites for ions. Bell et al.[41,43] have found that Cu can sit on a five- or six-membered ring, with preference toward the former. This is generally consistent with our finding that more than four oxygen atoms can coordinate with the copper. Additional work by Teraishi et al.[42] and Broclawik et al.[49] have shown that five-membered ring sites appear to be more stable for isolated Cu ionic species, while the formation of Cu−O−Cu bridges is more stable on six-membered ring sites containing at least two Al atoms. In addition, they have shown that this oxo species is more reactive than lone Cu for interaction with small molecules such as CO and NO.

Considering this information, it would be expected that the two low-temperature peaks in the TPR (Figure 1a) correspond to two different Cu sites on ZSM-5. Note the rate at which the Cu^{1+} peak is formed and the Cu−O coordination decreases in association with the first TPR peak, while the rate is subdued across the second peak. In addition, in examination of the range of shells between 3 and 5 Å typically associated with Cu−O−Cu bridging in the radial distribution plot in Figure 4, the presence of these shells appear to disappear near 175 °C, although, again, this change was not quantifiable. If, as stated above, the Cu−O−Cu species is more energetic, then it would be expected to react with H_2 at not only a lower temperature but at a faster rate as temperature is increased. Thus, we can tentatively assign the Cu_{4A} species as a state containing both isolated Cu^{2+} species on a five-membered ring and Cu^{1+} species in close proximity on the same six-membered ring. The transition from Cu_{4A} to Cu_{4B} would then be the reduction of the isolated Cu^{2+} species to Cu^{1+}; state Cu_{4B} would be then a combination of Cu^{1+} on both five- and six-membered rings. At temperatures above 375 °C, both species appear to be able to form Cu^0, but because the Cu^{1+} on six-membered rings are already in close proximity, it would be expected for these ions to easily sinter and form Cu clusters.

(49) Broclawik, E.; Datka, J.; Gil, B.; Kozyra, P. *Phys. Chem. Chem. Phys.* **2000**, *2*, 401−405.

In consideration of the CO TPR data, the possibility of two species may also be considered. At low temperatures near 200 °C, it would be expected for Cu−O−Cu to be more reactive to any reductant compared to isolated Cu^{2+} species, and would explain the somewhat larger decrease in the second Cu−O shell compared to the first. This species is still reactive to CO at moderate temperatures, and slowly reduced to Cu^{1+} by 450 °C. After 450 °C, the development of Cu^{1+} increases dramatically, suggesting that the isolated Cu^{2+} is reduced by CO at this point. This conclusion agrees with the findings of Kumashiro et al.,[5] who determined that at least two sites with different energetics existed for CO adsorption on Cu-ZSM-5. However, as we have previously noted, we were not able to separate out the interaction of Cu−O bonds from Cu−C bonds that would be expected to form during CO exposure on Cu-ZSM-5. The low-temperature reduction in coordination number may be also attributed to the desorption of CO from Cu species. We expect that future experimentation will be able to resolve the differences between the Cu−O and Cu−Cu bonds and to further qualify the changes in this system.

Conclusions

We have shown that the use of in situ XAFS to collect data with high-temperature resolution and high-energy resolution can be used to understand the changes in both oxidation state and the local environment of metallic atoms in heterogeneous catalysts. In particular, we have shown that Cu-ZSM-5, devoid of apparent CuO clusters, shows two species of isolated Cu ions, in agreement with other studies in the literature. These distinct species, bridging Cu−O−Cu and isolated Cu^{2+}, reduce in H_2 to Cu^{1+} at 175 and 205 °C, respectively. Reduction of Cu^{1+} occurs at 375 °C, with migration of the Cu species to form small Cu clusters. When Cu-ZSM-5 is exposed to CO, reduction of the oxo bridges appears to occur near 200 °C, while the isolated Cu^{2+} species are reduced near 450 °C.

Acknowledgment. Use of the Advanced Photon Source was supported by the U.S. Department of Energy, Basic Energy Sciences, Office of Science, under Contract No. W-31-109-Eng-38. Work performed at MR-CAT is supported, in part, by funding from the Department of Energy under Grant Number DEFG0200ER45811.

JA0176696